Supplementary Material

For

Organoclay-derived lamellar silicon carbide/carbon composite as an ideal support for Pt nanoparticles: facile synthesis and toluene oxidation performance

Runliang Zhu[a, b, c] *, Qingze Chen[a, b, c], Jing Du[a, b, c], Qiuzhi He[a, b, c], Peng Liu[d], Yunfei Xi[e], Hongping He[a, b, c]

[a] *CAS Key Laboratory of Mineralogy and Metallogeny, Guangdong Provincial Key Laboratory of Mineral Physics and Materials, Guangzhou Institute of Geochemistry, Chinese Academy of Sciences, Guangzhou 510640, China*

[b] *University of Chinese Academy of Sciences, Beijing 100049, China*

[c] *Institutions of Earth Science, Chinese Academy of Sciences, Beijing 100029, China*

[d] *School of Environment and Energy, South China University of Technology, Guangzhou 510006, China*

[e] *School of Earth, Environmental and Biological Sciences, Queensland University of Technology (QUT), Brisbane, QLD, 4001, Australia*

* Corresponding author

E-mail: zhurl@gig.ac.cn

Materials and methods

Materials

The original Mt (purity > 95%) used in this study was collected from Inner Mongolia, China. The chemical composition of Mt was given as follows: SiO_2 58.16%, Al_2O_3 16.95%, MgO 3.57%, Fe_2O_3 5.26%, CaO 2.29%, Na_2O 0.19%, K_2O 0.15%, TiO_2 0.20%, MnO 0.03%, P_2O_5 0.08%, and the loss on ignition was 13.12%. Crystal violet (CV, $C_{24}H_{28}N_3Cl$, analytical grade) and sodium chloride (NaCl, analytical grade) were bought from Shanghai Chemical Reagent Factory and Shanghai RichJoint Chemical Reagents Co Ltd, respectively. Magenisum power (Mg, analytical grade) and platinum nitrate solution (containing 18.02% Pt) were purchased from Shanghai Aladdin Chemical Reagent Co Ltd. Nitric acid (HNO_3, 68 wt.%), hydrochloric acid (HCl, 37 wt.%), and hydrofluoric acid (HF, 40 wt.%) were supplied by Guangzhou Chemical Reagent Factory, China.

Preparation of silicon carbide/carbon composite supported Pt catalyst

The preparation of Mt/carbon (Mt/C) composite: 5 g of Mt was added into a 500 mL of CV solution with a concentration of 4 g L^{-1}. The suspension was stirred vigorously for 6 h at 25°C, and then centrifuged to separate the solids. The CV was almost completely adsorbed on Mt, which was confirmed by the very low concentration of CV in the supernatant (meansured on an ultraviolet-visible spectrophotometer). The sediment (*i.e.*, organic Mt, denoted as Mt/CV) was dried at 60°C for 24 h. Then, the organic Mt was calcinated in a corundum tube furnace for 3 h at 650°C under a N_2 flow. The resulting

product (denoted as Mt/C) was collected for the following experiments after cooling down.

The preparation of SiC/C composite: Typically, 1 g of Mt/C, 0.7 g of Mg, and 5 g of NaCl were mixed uniformly, and transferred into a sealed stainless steel reactor. After being placed into the middle of a corundum tube furnace, the reactor was heated to 650°C at a ramp rate of 5°C min^{-1} and maintained for 3 h under a constant high-purity Ar flow. Subsequently, the obtained mixtures were rinsed with deionized water (to remove NaCl) and 1 mol/L HCl solution (to eliminate byproducts, *e.g.*, MgO and Mg_2Si), followed by leaching with 1 wt.% HF solution. The resulting SiC/C composite was washed thoroughly with ethylalcohol and deionized water, and vacuum-dried overnight at 60°C.

The preparation of Pt-loaded SiC/C (Pt-SiC/C) composite: Pt-SiC/C was synthesized *via* a simple impregnation method. 1 g of SiC/C was first dispersed in 5 mL 1 mol/L HNO_3 solution containing a certain amount of platinum nitrate solution, with the Pt loading amount of *x*% (*x* = 0.25, 0.5, and 1). The mixture was vigorously stirred for 1 h, and then heated to 250°C at a ramp rate of 1°C min^{-1} and held for 3 h under an Ar flow. According to the Pt loading amount of *x*%, the resulting Pt-SiC/C composite was denoted as *x*Pt-SiC/C (*x* = 0.25, 0.5, and 1).

Characterization methods

Powder X-ray diffraction (XRD) patterns of the samples were recorded using a Bruker AXS D8 Advance X-ray diffractometer with Ni-filtered CuKα radiation (λ = 0.154 nm) at 40 kV and 40 mA. Scanning electron microscope (SEM) images and energy

dispersive X-ray spectroscopy (EDS) were obtained using a Hitachi SU-8010 instrument. Transmission electron microscope (TEM) and high-resolution TEM (HRTEM) images were observed on an FEI Talos F200S field emission transmission electron microscope at an acceleration voltage of 200 kV. N_2 adsorption-desorption isotherms were measured at liquid nitrogen temperature (–196°C) on a Micromeritics ASAP 2020 system. The specific surface area was evaluated using the Brunauer–Emmett–Teller (BET) equation, and the total pore volume was estimated based on the N_2 adsorption capacity at relative pressure of 0.99. The pore size distribution (PSD) was calculated using the non-local density functional theory (NLDFT), which proven available for the size distributions of both micropore and mesopore.[1] X-ray photoelectron spectroscopy (XPS) results were collected on a Thermo Fisher K-Alpha XPS analyzer. XPS spectra were acquired using a monochromatic AlKα X-ray source (1468.6 eV), and pass energies for the survey scans and high-resolution scans were set as 100 and 30 eV, respectively. Hydrogen temperature-programmed reduction (H_2-TPR) tests were carried out on a DAS-7000 multifunctional automatic adsorption instrument. About 50 mg sample was heated from room temperature to 500 °C at a rate of 5 °C min^{-1} in a flowing 5% H_2/N_2 (30 mL min^{-1}).

Toluene catalytic oxidation measurements

The toluene catalytic oxidation performance of the catalyst was carried out in a fixed-bed reactor under atmospheric pressure in the temperature range of 100-250°C. 50 mg of catalyst (sieved to a particle size of 60-100 mesh) was loaded in the middle of a quartz tube microreactor (6 mm i.d.) on a quartz plate. The toluene vapor was generated

by flowing N_2 into toluene saturator (in an ice bath). The inlet gas consisted of 1000 ppm toluene and 20% O_2 adjusted by N_2. The total flow rate of feed stream was 50 mL min^{-1}, corresponding to a gas hourly space velocity (GHSV) of 60 000 $cm^3\ g^{-1}\ h^{-1}$. The concentration of CO_2 in outlet gas was measured by an on-line non-dispersive infrared CO_2 analyzer (GXH-3010E, Huayun, Beijing). The CO_2 generation was denoted as $(C/C_0) \times 100\%$, where C was the CO_2 concentration in outlet gas and C_0 was that when toluene was oxidized completely. Water was introduced into the feed stream *via* a syringe pump to investigate the effect of moisture (5% water) on the catalytic performance of the catalysts, and a heater attached on the gas line was used to avoid the condensation of water and toluene. The catalytic activities of the catalysts were estimated by the values of T10, T50, and T90, corresponding to the temperature at 10%, 50%, and 90% of CO_2 generation, respectively. The turnover frequency (TOF, s^{-1}) value of toluene on the catalyst was calculated based on the dispersion of Pt using the following equation:

$$TOF_{Pt} = X_{tol}F_{tol}M/m_{Cat}X_{Pt}D_{Pt}$$

Where X_{tol} represents the toluene conversion at certain temperature, F_{tol} (mol s^{-1}) denotes the flow rate of toluene, M (g mol^{-1}) is the molar mass of Pt, m_{Cat} (g) is the mass of catalyst, X_{Pt} is the mass fraction of Pt in the sample, and D_{Pt} is the dispersion of Pt (see Table S1).

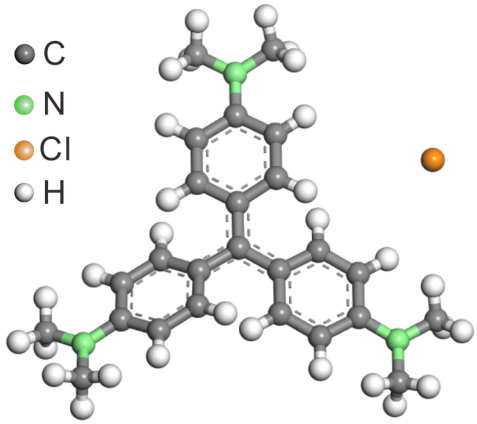

Fig. S1 The structure of cationic crystal violet.

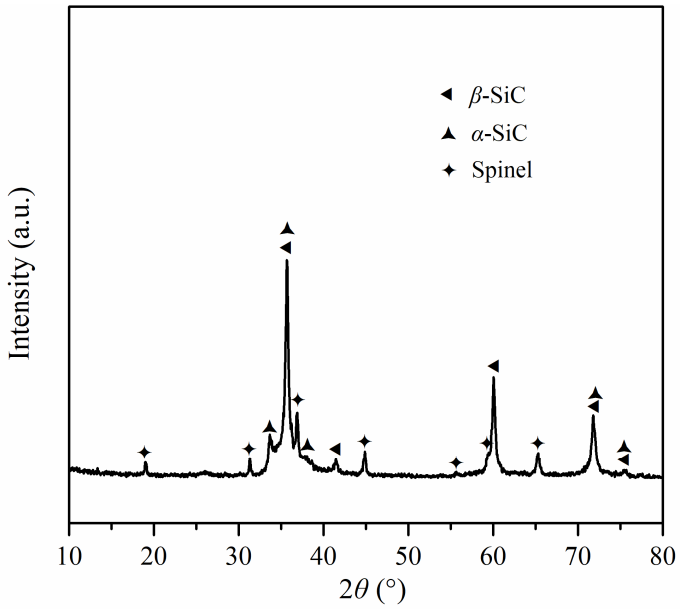

Fig. S2 XRD pattern of the final product after magnesiothermic reaction and acid washing using Mt/C as a precursor without the addition of NaCl.

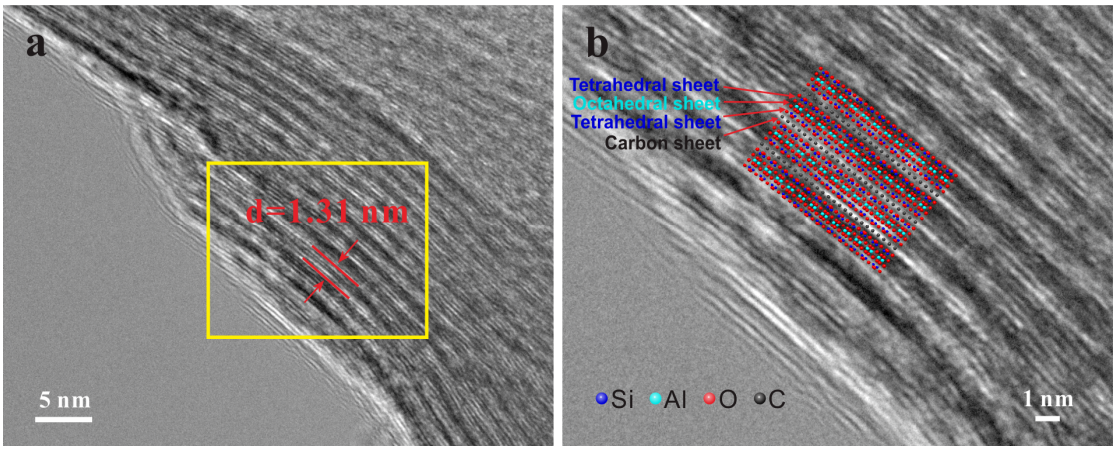

Fig. S3 HRTEM image (a) and the enlarged view along with a structural model (b) of Mt/C.

A sandwich structure consisting of Mt layer and carbon layer appeared in the HRTEM image of Mt/C (Fig. S3), which directly confirmed that the graphene-like sheet was *in situ* generated within the confined interlayer space of Mt.

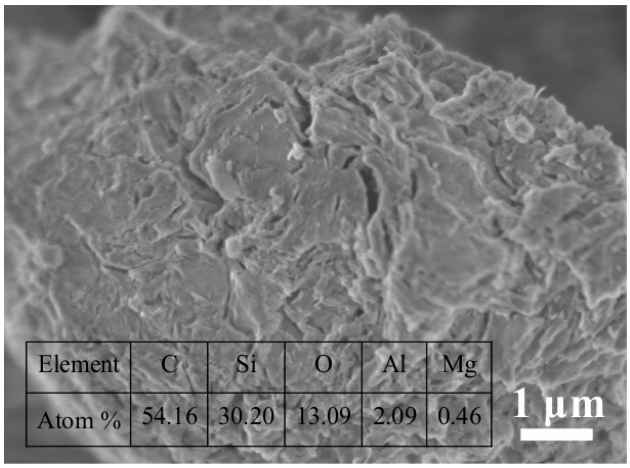

Fig. S4 SEM image and the corresponding EDS result of SiC/C.

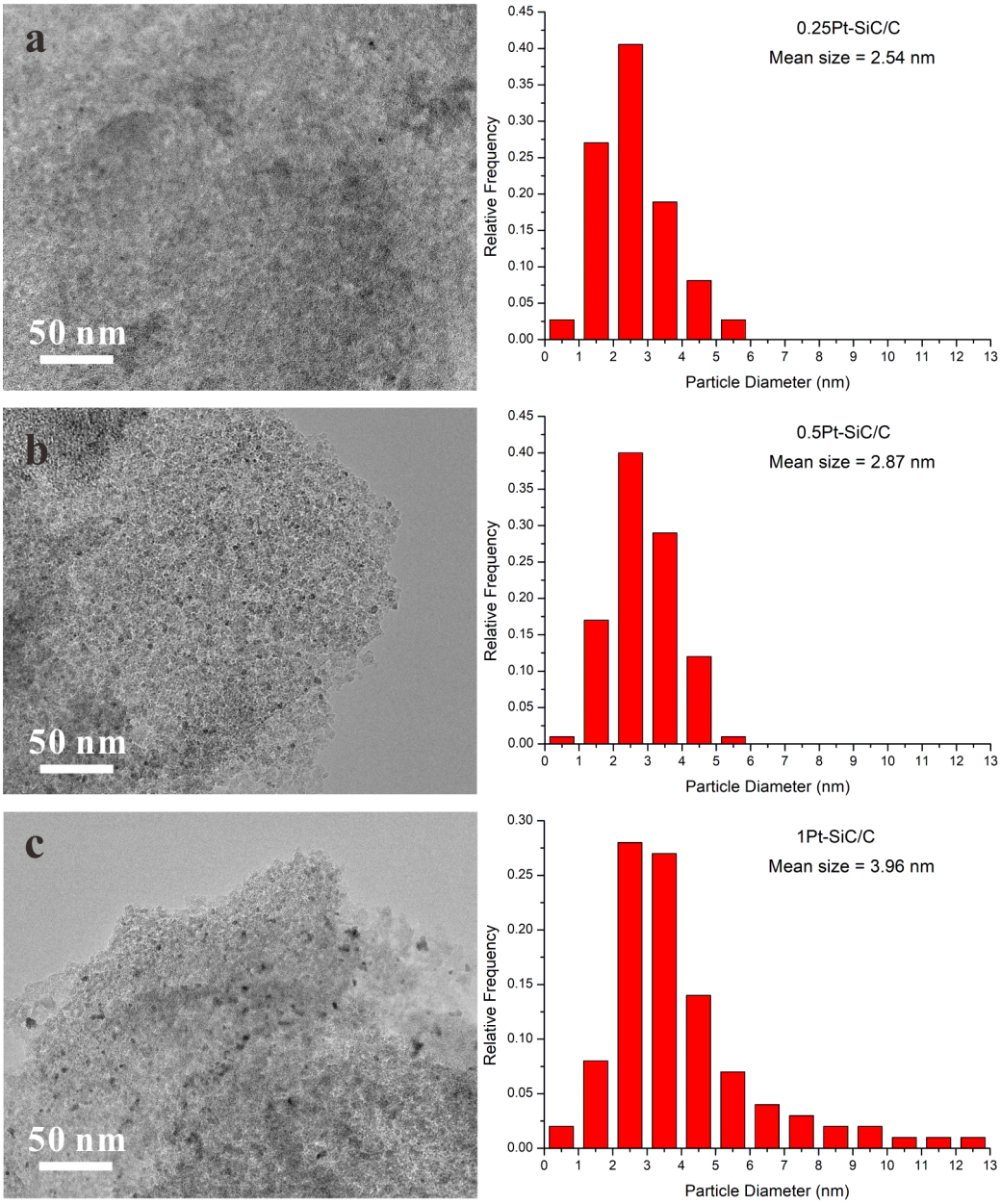

Fig. S5 TEM images and Pt particle size distributions of 0.25Pt-SiC/C (a), 0.5Pt-SiC/C (b), and 1Pt-SiC/C (c).

By randomly measuring the size of 50 Pt nanoparticles, the particle size distributions results showed that 0.25Pt-SiC/C and 0.5Pt-SiC/C possessed the smaller ranges of Pt particle size distribution (0.5-5.5 nm) than 1Pt-SiC/C (0.5-12.5 nm). With rising Pt loading amounts, the mean size of Pt increased and the dispersion of Pt nanoparticles decreased (Fig. S5 and Table S1).

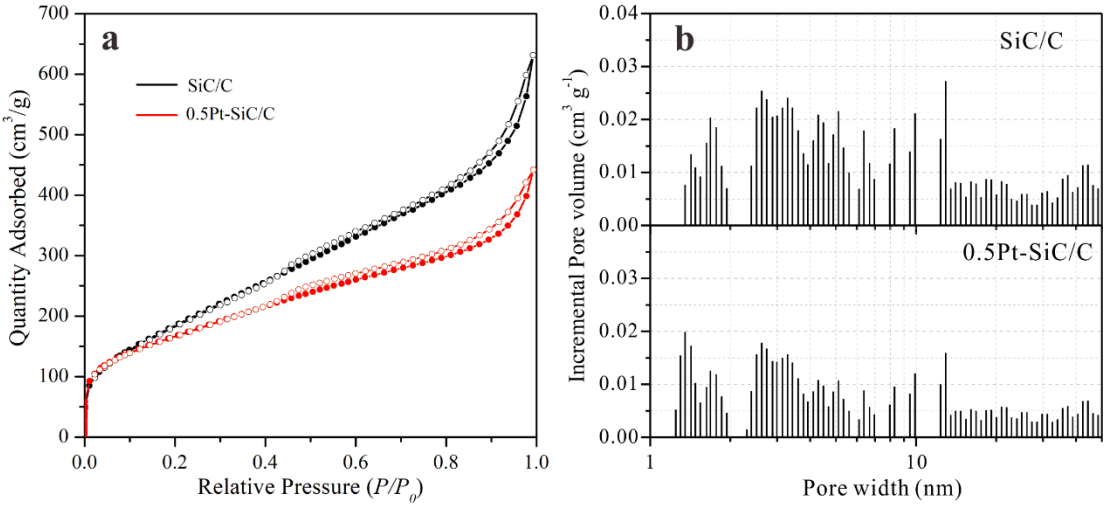

Fig. S6 N_2 adsorption-desorption isotherms (a) and pore size distribution patterns (b) of SiC/C and 0.5Pt-SiC/C.

The N_2 adsorption/desorption isotherms indicated that both SiC/C and 0.5Pt-SiC/C exhibited the characteristic II-type isotherms with H3-type hysteresis loops indicative of non-rigid slit-like pores (from the lamellar structure) (Fig. 3), according to the IUPAC Technical Report.[1] Noticeably, SiC/C could obviously adsorb N_2 at various relative pressures, suggesting the simultaneous presence of micro-, meso-, and macropores.The hierarchical porosity was favorable for the dispersion of Pt nanoparticles and the diffusion of the reactants and products (*e.g.*, in the catalytic reaction).[2]

The large surface area and hierarchically porous structure of Pt-loaded SiC/C could facilitate the diffusion/mass transfer, lowering the interception and deposition of byproducts on the catalyst surface.

Table S1 Textural parameters of various samples.

	Pt loading (%)	Pt mean size (nm)[a]	Pt dispersion (%)[b]
0.25Pt-SiC/C	0.25	2.54	44.1
0.5Pt-SiC/C	0.5	2.87	39.0
1Pt-SiC/C	1	3.96	28.3

[a] Determined by HRTEM.

[b] Calculated by the following equation:[3]

$$D_{Pt} = 600M/\rho daN_A$$

Where M represents the molar mass of Pt (195.08 g mol^{-1}), ρ is the density of metallic Pt (21.45 g cm^{-3}), d is the mean size of Pt particle observed from the HRTEM images, a denotes the surface area of Pt atom (8.06×10^{-20} m^2 $atom^{-1}$), and N_A is the Avogadro constant (6.02×10^{23} mol^{-1}).

Table S2 XPS results of various catalysts.

Samples	Pt $4f_{7/2}$ binding energy (eV)		Pt $4f_{5/2}$ binding energy (eV)		$Pt^0/(Pt^0+Pt^{2+})$
	Pt^0	Pt^{2+}	Pt^0	Pt^{2+}	
0.25Pt-SiC/C	71.9	73.7	75.4	77.1	0.51
0.5Pt-SiC/C	72.0	73.9	75.5	77.4	0.53
1Pt-SiC/C	71.8	73.8	75.2	77.3	0.49

Table S3 Catalytic performance of various catalysts for toluene oxidation.

Catalysts	CO_2 generation temperature (°C)			TOF_{Pt}[a] ($\times 10^{-3}$ s^{-1})
	T10	T50	T90	
SiC/C	-	-	-	-
0.25Pt-SiC/C	185	214	218	3.45
0.5Pt-SiC/C	158	181	184	8.37
1Pt-SiC/C	160	184	187	5.11

[a] The TOF values were calculated at 150°C.

Table S4 Catalytic performance for toluene oxidation over various supported Pt catalysts in this work and the recently reported studies.

Catalyst	Synthesis method	Pt loading (wt.%)	Toluene concentration (ppm)	Space velocity ($mL \cdot g^{-1} \cdot h^{-1}$)	Complete conversion temperature (T_{100}, °C)	Ref.
0.5Pt-SiC/C	Impregnation	0.5	1000	60000	185	This work
Pt/HPMOR	Impregnation	0.78	1000	60000	210	4
Pt/Beta-H zeolite	Impregnation	1	1000	60000	200	5
Pt/TiO_2	Impregnation	0.5	2000	34000	245	6
Pt/SiO_2	Impregnation	0.5	1000	60000	200	7
Pt/SiO_2	Oleic acid assisted impregnation	0.5	1000	60000	180	
Pt/Al_2O_3(S)	Impregnation	0.1	1000	24000	180	8
Pt/CeO_2	Impregnation followed by DBD plasma	0.77	200	50000	230	9
Pt/CeO_2-activated carbon	Impregnation	0.89	1000	40000	180	10
Pt/Al_2O_3-CeO_2	Ultrasound–plasma assisted impregnation	1	1300	12000	180	11
Pt/MnO_2	Hydrothermal method	0.1	100	48000	160	12

Reference:

1. M. Thommes, K. Kaneko, A. V. Neimark, J. P. Olivier, F. Rodriguez-Reinoso, J. Rouquerol and K. S. W. Sing, *Pure Appl. Chem.* , 2015, **87**, 1051-1069.
2. C. Chen, X. Wang, J. Zhang, C. Bian, S. Pan, F. Chen, X. Meng, X. Zheng, X. Gao and F.-S. Xiao, *Catal. Today* 2015, **258**, 190-195.
3. R. Peng, S. Li, X. Sun, Q. Ren, L. Chen, M. Fu, J. Wu and D. Ye, *Appl. Catal., B* 2018, **220**, 462-470.
4. J. Zhang, C. Rao, H. Peng, C. Peng, L. Zhang, X. Xu, W. Liu, Z. Wang, N. Zhang and X. Wang, *Chem. Eng. J.* , 2018, **334**, 10-18.
5. C. Chen, J. Zhu, F. Chen, X. Meng, X. Zheng, X. Gao and F.-S. Xiao, *Appl. Catal., B* 2013, **140-141**, 199-205.
6. X. Chen, Z. Zhao, Y. Zhou, Q. Zhu, Z. Pan and H. Lu, *Appl. Catal., A* 2018, **566**, 190-199.
7. H. Wang, W. Yang, P. Tian, J. Zhou, R. Tang and S. Wu, *Appl. Catal., A* 2017, **529**, 60-67.
8. T. Gan, X. Chu, H. Qi, W. Zhang, Y. Zou, W. Yan and G. Liu, *Appl. Catal., B* 2019, **257**, 117943.
9. B. Wang, B. Chen, Y. Sun, H. Xiao, X. Xu, M. Fu, J. Wu, L. Chen and D. Ye, *Appl. Catal., B* 2018, **238**, 328-338.
10. Z. Abdelouahab-Reddam, R. E. Mail, F. Coloma and A. Sepúlveda-Escribano, *Appl. Catal., A* 2015, **494**, 87-94.
11. F. Rahmani, M. Haghighi and P. Estifaee, *Microporous Mesoporous Mater.* , 2014, **185**, 213-223.
12. H. Zhang, S. Sui, X. Zheng, R. Cao and P. Zhang, *Appl. Catal., B* 2019, **257**, 117878.